Thermal Stability of Quaternary Phosphonium Modified Montmorillonites

Wei Xie,[†] Rongcai Xie,[†] Wei-Ping Pan,*,[†] Doug Hunter,[‡] Bryan Koene,[§]
Loon-Seng Tan,[∥] and Richard Vaia*,[∥]

*Thermal Analysis Laboratory, Material Characterization Center, Department of Chemistry,
Western Kentucky University, Bowling Green, Kentucky 42101; Southern Clay Products, Inc.,
1212 Church Street, Gonzales, Texas 78629; Triton Systems, Inc., 200 Turnpike Road,
Chelmsford, Massachusetts 01824; Air Force Research Laboratory/MLBP, Building 654,
2941 P Street, Wright-Patterson Air Force Base, Ohio 45433*

Organically modified layered silicates (OLS) with high thermal stability are critical for synthesis and processing of polymer layered silicate nanocomposites (PLSN). In the current study, the non-oxidative thermal degradation chemistry of alkyl and aryl quaternary phosphonium-modified montmorillonites (P-MMT) was examined using TGA combined with pyrolysis/GC-MS. The morphology evolution at elevated temperature was investigated using in-situ high-temperature X-ray diffraction (XRD) and Fourier transform infrared spectroscopy (FTIR). The onset decomposition temperature via TGA of these P-MMTs ranged from 190 to 230 °C. The initial degradation of the alkyl P-MMTs follows potentially two reaction pathways − β-elimination [E_β] and nucleophilic displacement at phosphorus [$S_N(P)$] − reflecting the multiple environments of the surfactant in the silicate. Aryl P-MMT decomposition proceeds via either a reductive elimination through a five-coordinate intermediate or radical generation through homologous cleavage of the P−phenyl bond. Overall, the interlayer environment of the montmorillonite has a more severe effect on stability of the phosphonium surfactant than previously reported for ammonium-modified montmorillonite (N-MMT). Nonetheless, the overall thermal stability of P-MMT is higher than that of N-MMT. These observations indicate that, in addition to their conventional purpose as stabilizers, phosphonium salts offer unique opportunities for melting processing polymer layered silicate nanocomposites.

Introduction

Nanocomposites have attracted substantial attention because of their superior physical and mechanical properties compared to those of their micro- and macro-composite counterparts containing an equivalent volume fraction of inorganic filler.[1] Exemplifying this class of materials are polymer layered silicate nanocomposites (PLSN), which have been shown to exhibit increased modulus,[2] increased solvent resistance,[3] decreased thermal expansion coefficient,[4] reduced gas permittivity,[4,5] self-passivation,[6] and reduced flammability[7] compared to those of the respective pristine polymer counterpart.

Optimal dispersion of the nano-constituent, such as montmorillonite (a commonly used layered silicate), in a polymer requires carefully chosen surface modification to lower the surface energy of the inorganic and to impart organophilicity. For montmorillonites and comparable layered silicates, this is achieved via an ionic exchange reaction between the naturally occurring alkali metal cations residing between the aluminosilicate layers and alkylammonium surfactants. However, the commonly used surfactants have limited thermal stability, in some cases less than the nominal processing temperature of the polymer resin. Furthermore, the elevated temperature interfacial chemistry complicates fundamental studies attempting to establish specific requirements for the montmorillonite/surfactant/polymer interface that is necessary for optimal dispersion and property enhancements.

Detailed degradation studies of alkyl and arylammonium modified montmorillonites (N-MMT) have been

* Authors to whom correspondence should be addressed. R. A. Vaia: phone 937-255-9184; fax 937-255-9157; e-mail richard.vaia@wpafb.af.mil. W.-P. Pan: phone 270-780-2532; fax 270-782-8226; e-mail wei-ping.pan@wku.edu.
† Western Kentucky University.
‡ Southern Clay Products.
§ Triton Systems.
∥ AFRL/MLBP.

(1) Vaia, R. A.; Giannelis, E. P. *MRS Bull.* **2001,** *26* (May), 394.
(2) Kojima, M.; Usuki, A.; Okada, A.; Kamigato, O. *J. Mater. Res.* **1993,** *8,* 1185. Messersmith, P. B.; Giannelis, E. P. *Chem. Mater.* **1994,** *6,* 1719. Lan, T.; Pinnavaia, T. *J. Chem. Mater.* **1994,** *6,* 216. Wang, M. S.; Pinnavaia, T. *J. Chem. Mater.* **1994,** *6,* 648.
(3) Burnside, S. D.; Giannelis, E. P. *Chem. Mater.* **1995,** *7,* 1597. Huang, J.; Zhu, Z.; Yin, J.; Qian, X.; Sun, Y. *Polymer* **2000,** *42,* 873.
(4) Yano, K.; Usuki, A.; Kamigaito, O. *J. Polym. Sci., Part A: Polym. Chem.* **1993,** *31,* 2493. Yano, K.; Usuki, A.; Okada, A. *J. Polym. Sci.: Part A: Polym. Chem.* **1997,** *35,* 2289.
(5) Messersmith, P. B.; Giannelis, E. P. *J. Polym. Sci., Part A: Polym. Chem.* **1995,** *33,* 1047.

(6) Vaia, R. A.; Price, G.; Ruth, P. N.; Nguyen, H. T.; Lichtenhan, J. *Appl. Clay Sci.* **1999,** *15* (*1*), 67.
(7) Gilman, J. W.; Jackson, C. L.; Morgan, A. B.; Harris, R. H.; Manias, E.; Giannelis, E. P.; Wuthenow, M.; Hilton, D.; Phillips, S. *Chem. Mater.* **2000,** *12,* 1866.

recently reported.[8-13] Initial degradation of the ammonium surfactant generally proceeds by a Hofmann (β-elimination) process, which depends on the basicity of the anion, the steric environment around the ammonium, and temperature.[8] However, when present in the montmorillonite, additional mechanisms, such as nucleophilic substitution, are observed.[9-11] The multiple pathways are attributed to a fraction of excess (unexchanged) surfactant and the chemically heterogeneous morphology of the layered silicate.[9,14] Catalytic sites on the aluminosilicate layer reduce the thermal stability of a fraction of the surfactants by an average of 15-25 °C. Depending on the analysis technique and procedure employed, the onset temperature of nonisothermal degradation varies between 165 and 200 °C.[9-11] Finally, the release of organic compounds is staged and is associated with retardation of product transfer arising from the pseudo-two-dimensional morphology of the montmorillonite.[9,12] Recent NMR studies confirm that degradation of the surfactant can occur during compounding.[13] The recognition of the catalytic role of the aluminosilicate and the morphological influence on product evolution implies that the specific reaction details and the onset temperature will depend markedly on the source of the aluminosilicate, the anion of the ammonium salt,[14] workup history of the N-MMT, and the extent of dispersion within the polymer, and not simply the size of the intercalate.

Numerous concepts have been proposed that offer alternatives to conventional N-MMT when thermal limitations are a concern. These include emulsion and suspension polymerization in which unmodified (alkali-metal-containing) montmorillonite is used;[15] sol/gel technology which consists of a direct crystallization of organically modified layered silicates by hydrothermal treatment with a gel containing organics and organometallics;[16] partial exchanged systems which decrease the volume fraction of surfactant needed;[17] utilization of montmorillonite charged balanced by protons (so-called proton clays);[18] utilization of alkyl imidazolium as the surfactant to increase the initial decomposition temperature;[19] and utilization of phosphonium-based surfactants to improve the thermal stability.[11,20]

Phosphonium compounds are widely used as stabilizers in many applications and offer unique additional opportunities for polymer-layered silicate nanocomposites.[21] For example, mono- and bisphosphonium salts are used as flame retardants for textiles and paper, stabilization agents for polyacrylonitrile fibers exposed to sunlight, heat stabilizers for nylon, and condensation additives to organic dyes to produce wash-fast colors. Thus, the use of phosphonium salts as organic modifiers to layered silicates may further enhance the thermal and flammability properties of polymer nanocomposites.

To provide a better understanding of the thermal behavior of phosphonium salts and their modified montmorillonites (P-MMT), this article will discuss the thermal stability and degradation mechanism of phosphonium-modified montmorillonite, and compare them to those of ammonium-modified montmorillonites.

Experimental Section

Materials. Phosphonium montmorillonites (P-MMT) were fabricated following conventional procedures established for alkylammonium exchanged montmorillonites.[22] In brief, the quaternary phosphonium or ammonium salt is added to a purified montmorillonite slurry, then the flocculated product is removed by filtration, dried, and milled. To evaluate the P-MMTs with regard to commercial processing, additional Soxhlet extraction to remove excess, unexchanged surfactant was not performed. It has been demonstrated in previous studies that this procedure influences the degradation profile.[9] The quaternary ammonium and phosphonium surfactants and resulting organically modified montmorillonites, milli-equivalent exchange ratio (MER), and interlayer distance (d_{001}) are detailed in Table 1. Tributyltetradecyl phosphonium bromide was used as received from Cytec Industries, Inc. and all other surfactants were used as received from Aldrich Inc. Na$^+$ Montmorillonite (Cloisite Na$^+$; cation exchange capacity, CEC = 92 meq/100 g; mean formula unit Na$_{0.65}$[Al,Fe]$_4$Si$_8$O$_{20}$(OH)$_4$) was provided by Southern Clay Products, Inc.

Thermal Characterization. Thermogravimetric analysis (TGA) was conducted on a TA Instruments TGA2950 using an ultrahigh purity (UHP) nitrogen atmosphere, heated from room temperature to 1000 °C (2 and 5 °C/min). TGA was calibrated with indium, tin, zinc, and silver (heating rate 2 °C/min, the melting point was determined from dT/d$t(T)$). The standard error, σ, for T_{onset} and T_{max} is 1.5 and 1 °C, respectively. Total fraction of organic in the OLS was determined by adjusting the total mass loss from 150 to 1000 °C with the mass loss of the parent Na$^+$-montmorillonite from 450 to 700 °C (5.48%) to account for the mass loss associated with dehydroxylation of the aluminosilicate.[9] These values agreed with those determined from loss on ignition for selected samples.

Onset temperatures were determined by TGA experiments as the point where the derivative weight loss is 0.001%/°C over

(8) Cope, A. C.; Trumbull, E. R. In *Organic Reactions 11*; John Wiley and Sons: New York, 1960; pp 317–487. March, J. *Advanced Organic Chemistry, Reactions, Mechanisms and Structures*, 4th ed.; John Wiley and Sons: New York, 1992; pp 982, 999–1001. Sokal'skaya, L. I.; Semenov, V. A.; Osipova, E. S.; Zhukova, N. G. *USSR Zh. Prikl. Khim. (Leningrad)* **1987**, *60* (5), 1127–32.

(9) Xie, W.; Pan, W.-P.; Hunter, D.; Vaia, R. *Chem. Mater.* **2001**, *13*, 2979.

(10) Zanetti, M.; Camino, G. In *The Proceedings of Tenth International Conference − Additives 2001*; Hilton Head Island, South Carolina, 2001; ECM, Inc.: Plymouth, MI, 2001; pp 1–9.

(11) Zhu, J.; Morgan, A. B.; Lamelas, F. J.; Wilkie, C. A. *Chem. Mater.* **2001**, *13*, 3774. Fajnor, V. S.; Hlavaty, V. *J. Therm. Anal. Calorim.* **2002**, *67*, 113.

(12) Nyden, M. R.; Gilman, J. W. *Comput. Theor. Polym. Sci.* **1997**, *7*, 191.

(13) Vanderhart, D. L.; Asano, A.; Gilman, J. W. *Chem. Mater.* **2001**, *13*, 3796.

(14) The thermal stability of quaternary alkylammonium salts depends on the basicity of the anion.[8] Initial results for hexyldecyl trimethyl exchanged montmorillonites fabricated from the chloride and bromide salts showed a decrease in thermal stability of the OLS as the bascicity of the anion increased (Br$^-$ 152 °C, Cl$^-$ 168 °C). Correspondingly, no change in the general decomposition profile or total mass loss was observed. This indicates that unexchanged surfactant and subsequent decomposition products may also contribute to the initial decomposition of the OLS.

(15) Rossi, G. B.; Beaucage, G.; Dang, T. D.; Vaia, R. A. *Nano Lett.* **2002**, *2*, 319. Huang, X.; Brittain, W. J. *Macromolecules* **2001**, *34*, 3255.

(16) Mark, J. E. *Polym. Eng. Sci.* **1996**, *36*, 2905. Carrado, K. A.; Xu, L. *Chem. Mater.* **1998**, *10*, 1440. Ukrainczyk, L.; Bellman, R. A.; Anderson, A. B. *J. Phys. Chem. B* **1997**, *101*, 531.

(17) Ijdo, W. L.; Pinnavaia, T. J. *J. Solid State Chem.* **1998**, *139*, 281.

(18) Lan, T.; Kaviratna, P. D.; Pinnavaia, T. J. *J. Phys. Chem. Solids* **1996**, *57*, 1005.

(19) Gilman, J. W.; Morgan, A. B.; Harris, R. H.; Trulove, P. C.; DeLong, H. C.; Sutto, T. E. *Polym. Mater. Sci. Eng.* **2000**, *83*, 59. Gilman, J. W.; Awad, W. H.; Davis, R. D.; Shields, J.; Harris, R. H., Jr.; Davis, C.; Morgan, A. B. Sutto, T. E.; Callahan, J.; Trulove, P.; DeLong, H. C. *Chem. Mater.* **2002**, *14*, (in press).

(20) Yeh, J. M.; Liou, S. J.; Lin, C. Y.; Cheng, C. Y.; Chang, Y. W.; Lee, K. R. *Chem. Mater.* **2002**, *14*, 154.

(21) Kosolapoff, G. M.; Maier, L. *Organic Phosphorus Compounds*, Vol 2; John Wiley & Sons: New York, 1972.

(22) Vaia, R. A.; Teukolsky, R. K.; Giannelis, E. P. *Chem. Mater.* **1994**, *6*, 1017.

Table 1. Properties and Relative Mass Loss (TGA) during Decomposition of the P-mmt

sample	surfactants[a]	milli-equivalent exchange ratio, MER (meq/100 g)	d_{001} (nm)	% mass loss[b]			% total organic
				<120 °C	120−500 °C	first event	
P-C12	TPhDPBr	95	1.82	0.55	21.72	11.38	27.14
P-C14	TBTPBr	95	1.93	0.49	25.35	8.04	25.50
P-C16	TBHPBr	95	2.04	0.53	26.24	9.84	26.49
P-C18	TBOPBr	95	2.18	0.41	36.98	21.82	37.13
P-4Ph	TPhPBr	95	1.88	1.89	15.29	7.97	25.66
P-4C8	TOPBr	95	2.20	0.45	22.11	7.98	24.71
N-4C8	TONBr	95	2.21	0.47	24.97	8.62	27.08

[a] TPhDPBr, triphenyldodecyl phosphonium bromide; TBTPBr, tributyltetradecyl phosphonium bromide; TBHPBr, tributylhexadecyl phosphonium bromide; TBOPBr, tributyloctadecyl phosphonium bromide; TPhPBr, tetraphenyl phosphonium bromide; TOPBr, tetraoctyl phosphonium bromide; TONBr, tetraoctylammonium bromide. [b] First event refers to first organic decomposition peak corresponding to mass loss between $T_{onset,1}$ and $T_{onset,2}$ (see Table 2 for definition).
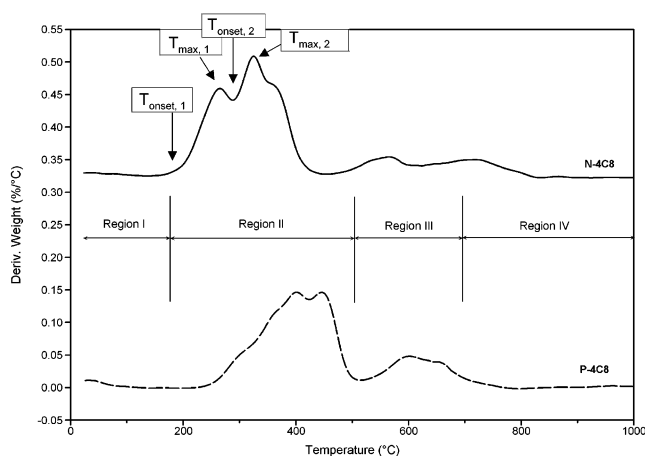

Figure 1. DTG (derivative weight loss) curves comparing quaternary ammonium montmorillonite (N-4C8) and quaternary phosphonium montmorillonite (P-4C8).

the value of the lower-temperature, steady state, plateau (heating rate of 2 °C/min in UHP nitrogen atmosphere). Pyrolysis/GC-MS experiments were carried out on a Pegasus II GC/MS system, which included a time-of-flight mass spectrometer and a high-speed gas chromatograph. The detailed instrumental setup description can be found elsewhere.[23]

Morphology Characterization. Standard wide-angle X-ray diffraction data were collected on powders using a THERMO-ARL Scintag X'TRA X-ray diffractometer with Cu K$_\alpha$ radiation at a scanning rate of 1°/min. In-situ, high-temperature X-ray diffraction experiments were also carried out on the THERMO-ARL Scintag X'TRA X-ray diffractometer with a high-temperature chamber with a heating rate of 5 °C/min.

In-situ, elevated-temperature FTIR experiments were conducted on an AABSPEC 2000 multi-mode experimental chamber coupled with a Perkin-Elmer 2000 series infrared spectrometer with a nominal resolution of 4 cm^{-1}. Spectra were recorded continuously as the samples were heated from room temperature to 500 °C at a heating rate of 5 °C/min. Peak area for $\nu_{as}CH_2$, ν_sCH_2, $\nu_{as}CH_3$, and ν_sCH_3 where determined from a nonlinear least squares deconvolution (Genplot, CGS, Inc.) of the features between 2800 and 3100 cm^{-1} by four Pearson VII curves.

Results

Thermal Stability of P-MMTs. Nonisothermal decomposition of quaternary phosphonium modified montmorillonite (Figure 1, e.g., tetraoctyl phosphonium modified montmorillonite) can be conveniently considered in four regions, overall similar to that observed for quaternary ammonium modified montmorillonite (Figure 1; e.g., tetraoctylammonium modified montmorillo-
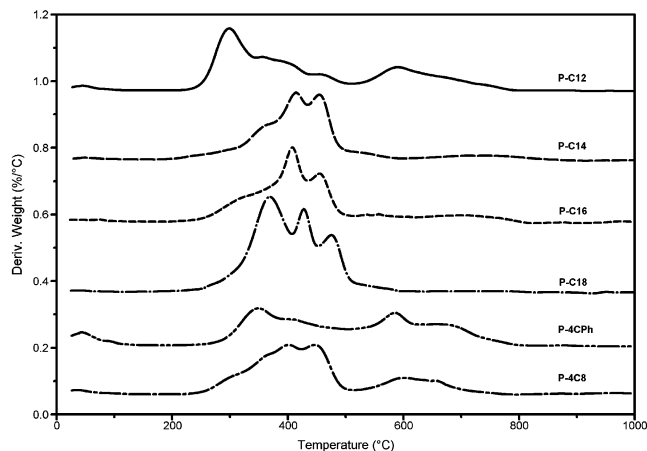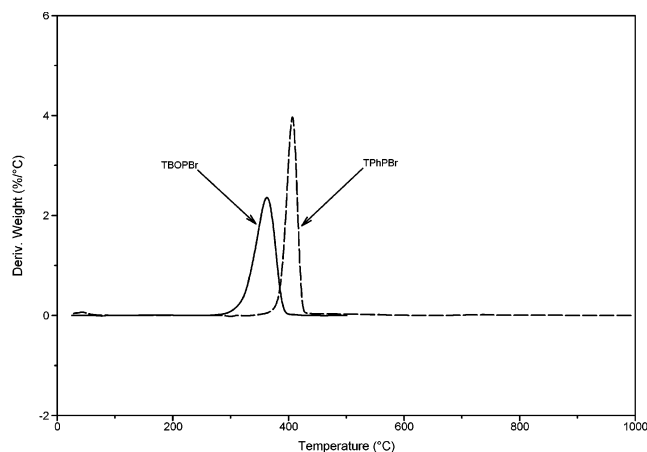
(23) Xie, W.; Pan, W.-P. *J. Therm. Anal. Calorim.* **2001**, *13*, 2979.

Figure 2. (a) DTG curves from TGA for quaternary phosphonium bromides (TBOPBr and TPhPBr). (b) DTG curves from TGA of quaternary phosphonium montmorillonites (P-C12, P-C14, P-C16, P-C18, P-4Ph, and P-4C8).

nite). Briefly, evolution of absorbed water and gaseous species, such as physiabsorbed CO_2 and N_2, occurs below 180 °C (Region I). Organic substances evolve from 250 °C to 500 °C (Region II). Dehydroxylation of the aluminosilicate occurs from 500 °C to 700 °C (Region III), and evolution of products associated with residual organic carbonaceous residue occurs between 700 °C and 1000 °C (Region IV). The most important regions influencing the PLSN service environment are Region I and II, where the release of small molecules associated with fabrication and storage of the P-MMT or the evolution of decomposition products may modify interfacial energies between the silicate and polymer.

Figure 2a and b summarizes the derivative thermogravimetry (DTG) curves of two phosphonium surfac-

Table 2. Decomposition Temperatures in Ultra-High Pure N_2

	TGA, °C			
	$T_{onset,1}$	$T_{max,1}$	$T_{onset,2}$[a]	$T_{max,2}$[b]
	P-MMT			
P-C12	210 (215[c])	301	341	355
P-C14	192 (188[c])	367	383	415
P-C16	193 (191[c])	321	382	408
P-C18	196 (181[c])	369	407	429
P-4Ph	230 (230[c])	347	386	409
P-4C8	226 (227[c])	360	377	446
TBTPBr	252	363		
TBOPBr	262	363		
TPhPBr	309	407		
TOPBr	262	362		
	N-MMT			
N-4C8	162 (157[a])	266	289	327
TONBr	170	212		

[a] $T_{onset,2}$ refers to peak valley temperature between 1st peak and 2nd peak in DTG. [b] $T_{max,2}$ refers to peak maximum temperature of 2nd DTG peak. [c] Onset temperature determined before predrying OLS at 140 °C.

tants (tetraphenyl phosphonium bromide and tributyloctadecyl phosphonium bromide) and six quaternary phosphonium montmorillonites (P-C12, P-C14, P-C16, P-C18, P-4Ph, and P-4C8). Table 1 summarizes the relative mass loss at various temperatures for the modified montmorillonites. Although the decomposition temperature varied for the different phosphonium salts, single-step decomposition is clearly observed. In contrast, the surfactant within the montmorillonite exhibits three to four discrete events in which the first event accounts for 30−50% of the total organic mass loss, depending on the P-MMT. The multiple events are attributed to the nanoscopic dimensions of the interlayer influencing the reaction kinetics, product transfer, and volatilization. For example, previous studies have shown that the rate and magnitude of the mass loss associated with the first event depends on process history, N-MMT morphology, and excess surfactant.[9] This event does not simply reflect the quantity of excess surfactant, as the relative mass loss is substantially greater than the amount of excess surfactant (∼1−2%). Overall though, the complex interplay of process history and interdependence of the characteristics of the various decomposition events necessitates further study before specific aspects of each event are understood.

Table 2 summarizes the onset temperatures and temperature at maximum rate of mass loss for the P-MMTs, using the procedure established in the previous study.[9] A pre-anneal at 140 °C was necessary to remove physiabsorbed water and gases to ensure a reproducible estimate of the onset temperature. The onset temperature and maximum rate of mass loss for the phosphonium surfactants are consistently 70−80 °C higher than those of the first events in the P-MMT as qualitatively observed in Figure 2b. The decrease in the thermal stability of the surfactant has been attributed to the presence of Lewis and Brønsted acid sites within the aluminosilicate layer.[9] Note that these studies indicated that the onset decomposition temperature determined by the initial deviation of the DTG curve from baseline underestimates the decomposition onset determined by the initial appearance of decomposition products in MS-TGA. Thus, qualitative comparison of onset temperatures necessitates similar experimental
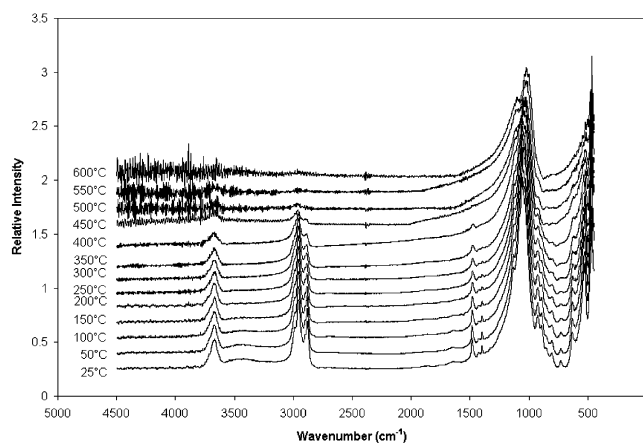
Figure 3. Temperature-dependent FTIR evolution spectra for P-C18.

technique and these values serve as a lower-bound estimate for nonisothermal stability.

Thermal-IR-spectroscopy was used to examine the structure evolution of P-MMT, providing information complementary to that of TGA with regards to the chemical aspects of the solid residue. Figure 3 illustrates the temperature-dependent IR spectrum profiles for P-C18. The absorption spectra of layered silicates have been broadly surveyed.[24] In brief, structural OH groups exhibit absorption at 3600 to 3700 cm^{-1}, whereas the water shows adsorption at lower frequencies, 3400 and 1640 cm^{-1}. Frequencies between 1150 and 400 cm^{-1} are described as "lattice vibration".[24] The absorption at 1062 and 1054 cm^{-1} is attributed to Si−O in-plane vibration. Absorption bands at 926, 896, and 802 cm^{-1} are attributed to R−O−H bending vibration. The strong absorption in the region below 550 cm^{-1} arises principally from in-plane vibrations of octahedral ions and their adjacent oxygen layers.[25]

For the aluminosilicate layer, the structural OH groups, apparent by the O−H stretching at 3675 cm^{-1} and R−O−H bending at 926, 896, and 802 cm^{-1}, are resolved up to 500 °C. The disappearance of hydroxyls is attributed to the destruction of the octahedral layer via dehydroxylation of the crystal structure.[24] Absorbed water content, associated with the broad absorption at 3400 and 1640 cm^{-1}, gradually decreases with increasing temperature and disappears at 250 °C. Finally, bands observed between 3000 and 2800 cm^{-1} (CH_2 and CH_3 stretching) and at 728 cm^{-1} (($CH_2)_n$ rocking) are associated from alkyl groups, decrease in intensity, and disappear at around 500 °C.

The relative change in the absorbance of a band is proportional to the relative concentration of the chemical moiety. Figure 4 compares the DTG data for P-C18 to the relative change in the total area of the asymmetric and symmetric CH_2 and CH_3 vibrations (heating rate for both thermal FTIR and TGA is 5 °C/min). Note that because vibronic bands are broadened by increased temperature, total area of the absorbance is more reflective of relative compositional change than the absorbance maximum. The thermal-IR results show a

(24) Farmer, V. C.; Russell, J. D. *Spectrochim. Acta* **1964**, *20*, 1149. Miller, G. J. *J. Phys. Chem.* **1961**, *65*, 800. Percival, H. J.; Ducan, J. F.; Foster, P. K. *J. Am. Ceram. Soc.* **1974**, *57*, 57.
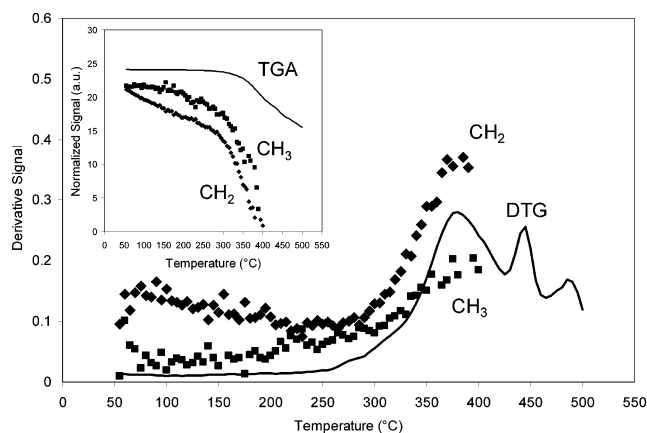(25) Grim, R. E. *Clay Minerals*; McGraw-Hill: New York, 1968.

Thermal Stability of Modified Layered Silicates

Chem. Mater., Vol. 14, No. 11, 2002 **4841**

Figure 4. Comparison of the relative rate of change (derivative) of the mass loss (DTG) and peak area (FTIR: $CH_2 = \nu_{as}CH_2$ and $\nu_s CH_2$; $CH_3 = \nu_{as}CH_3$ and $\nu_s CH_3$) for P-C18. The relative temperature dependence of the magnitudes is displayed in the inset.
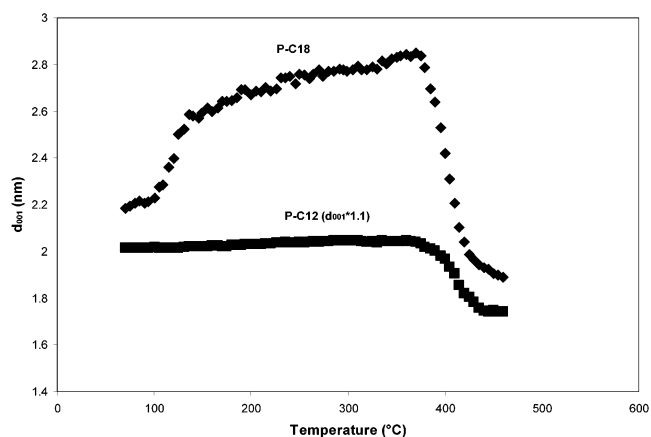

Figure 5. Change of layer distance (d_{001}) as a function of temperature from in-situ high-temperature X-ray diffraction for P-C12 and P-C18.

temperature dependent trend similar to that of the DTG data with an onset temperature of approximately 300 °C (note that the heating rate is greater than that discussed in Tables 1 and 2). Resolvable peaks in the FTIR are present only up to ~400 °C and are absent for the higher temperature events observed in the DTG.[26] These higher events account for ~50% of the organic mass loss, implying that the organic mass remaining after the first DTG event is carbonaceous residue devoid of alkanes. This is a substantial char yield for simple alkanes, again reflecting the influence of the nanoscopic dimensions of the layered silicate on the thermal degradation characteristics.

The subsequent decomposition of the carbonaceous char occurs during the higher-temperature DTG events as well as during Region III and IV (Figure 1). The relative amount of char retained above 500 °C (Table 1: difference between % mass loss from 120 to 500 °C and % total organic content) depends directly on the architecture of the phosphonium surfactant, where increased content of higher char-yielding aromatic moieties lead to greater char retention within the P-MMT at higher temperatures. Above 500 °C, tributyl alkyl P-MMTs contain ~1–2% residual, tetraoctyl P-MMT contains ~8%, triaryl alkyl P-MMT contains ~22%, and tetraphenyl P-MMT contains ~40%.

In-situ X-ray diffraction of the decomposition process is shown in Figure 5 for P-C12 and P-C18. The initial increase in layer repeat distance (d_{001}) for P-C18 has been attributed to a melting transition of the intercalated surfactant between 70 and 100 °C.[22,28] Note that

the magnitude of initial increase in d_{001} for P-12 is relatively smaller than that for P-18. Previous FTIR and NMR studies[22,28] indicate that short chain length and high temperature favor the disordered conformation. Therefore, the transition from an ordered conformation at room temperature to a disordered state at higher temperature is more noticeable for P-18C than for P-12C, resulting in a more obvious increase in d_{001} between 70 and 100 °C. Above 100 °C, gallery height increases monotonically to ~370 °C, which is comparable to the maximum rate of mass loss in TGA and maximum rate of absorption change in FTIR. Above 370 °C, the gallery height starts to decrease with increasing temperature, indicating the collapse of the interlayer gallery. This is substantially higher than the onset of thermal decomposition and comparable to the temperature of maximum rate of mass loss. These results suggest that the products from the initial decomposition process are retarded and trapped, and that the restriction of volatiles suffices to create an internal pressure that maintains the interlayer distance even though mass is evolving.

Thermal Degradation Mechanism of P-MMT. Pyrolysis products determined by pyrolysis/GC–MS from P-18C, P-4Ph, and their corresponding phosphonium salts at temperatures of 250, 300, 350, and 400 °C are summarized in Table 3. A step-by-step degradation pathway can be derived from the product distribution at the different temperatures. The decomposition behavior of the alkyl phosphonoium montmorillonites, such as P-12C, is very similar to that of P-18C.

Because of the greater steric tolerance of the phosphorus atom and the participation of its low-lying d-orbitals in the processes of making and breaking chemical bonds, phosphonium salts are generally capable of undergoing a wider range of reactions and behave differently than their ammonium counterparts toward an external base (*B*). The following types of reactions have been established for tetraalkyl phosphonium salts under appropriate conditions, Scheme 1:[29] (1) Nucleophilic substitution reaction at the α-carbon center,[30] **[S_N(C)]**: where the attendant nucleophilic

(26) Comments on resolution of FTIR. Alkanes fragments of different lengths cannot be differentiated on the basis of IR spectra because they exhibit the same C–H stretching and deformation frequencies. C=C stretching vibration (1680–1620 cm⁻¹) from alkenes (one of the products from decomposition of surfactant) are not observed in the IR spectrum, because in contrast to the strong C–H absorption, the C=C stretching vibration gives rise only to weak bands in the infrared in nonconjugated compounds.[27] This, together with the relatively low local concentration of OLS (KBr/OLS = 50:1) which in turn produce even less alkenes, results in insufficient resolution in IR to pick out the C=C bond.

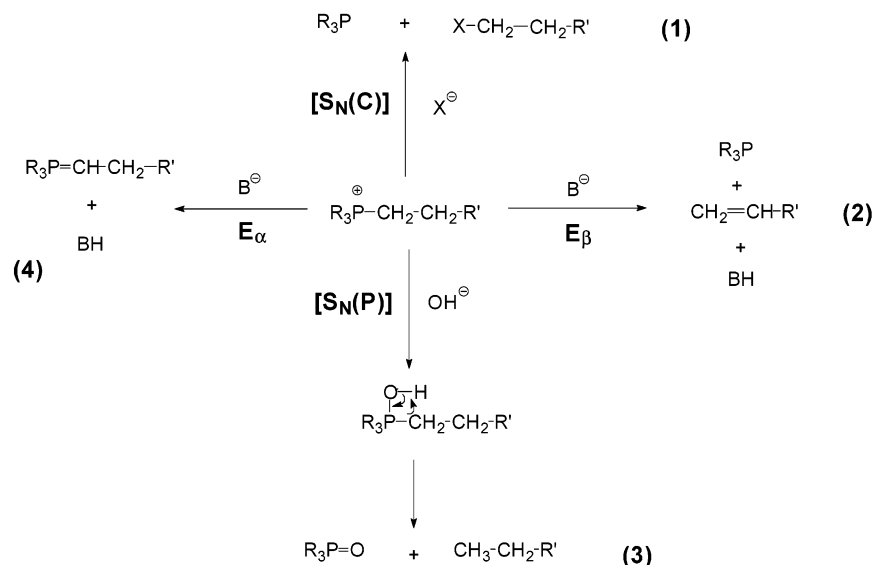(27) Bellamy, L. J. *The Infrared Spectra of Complex Molecules*; John Wiley & Sons: New York, 1960.

(28) Wang, L.-Q.; Liu, J.; Exarhos, G. J.; Flanigan, K. Y.; Bordia, R. *J. Phys. Chem. B* **2000**, *104*, 2810. Hackett, E.; Manias, E.; Giannelis, E. P. *Chem. Mater.* **2000**, *12*, 2161.

(29) Hudson, R. F. *Structure and Mechanism in Organo-Phosphorus Chemistry*; Academic Press: New York, 1965; pp 204–249.

(30) Fenton, G. F.; Hey, L.; Ingold, C. K. *J. Chem. Soc.* **1933**, 989.

Table 3. Representative Organic Species Evolved from P-C18 and TBOPBr (Pyrolysis/GC−MS)

	250 °C	300 °C	350 °C	400 °C
		P-C18		
alkane, linear	$C_{18}H_{38}$	C_8H_{18}, C_9H_{20}, $C_{13}H_{28}$, $C_{16}H_{34}$,	C_8H_{18}, C_9H_{20}, $C_{12}H_{26}$, $C_{13}H_{28}$, $C_{17}H_{36}$,	$C_{10}H_{22}$, $C_{12}H_{26}$, $C_{13}H_{28}$, $C_{17}H_{36}$
alkane, branched	decane, 2,5,9-trimethyl- [$C_{13}H_{28}$]	tridecane, 4-methyl- [$C_{14}H_{30}$]	tridecane, 4-methyl- [$C_{14}H_{30}$]	tridecane, 4-methyl- [$C_{14}H_{30}$] hexane, 2,4-dimethyl- [C_8H_{18}]
phosphine	$C_{12}H_{27}P$	$C_{12}H_{27}P$	$C12H_{27}P$	$C_{12}H_{27}P$
phosphine oxide	$C_{12}H_{27}OP$	$C_{12}H_{27}OP$	$C_{12}H_{27}OP$	$C_{12}H_{27}OP$
linear alkene, 1-	$C_{12}H_{24}$, $C_{13}H_{26}$, $C_{14}H_{28}$, $C_{18}H_{36}$	$C_{12}H_{24}$, $C_{13}H_{26}$, $C_{14}H_{28}$, $C_{17}H_{34}$, $C_{18}H_{36}$	C_7H_{14}, C_8H_{16}, C_9H_{18}, $C_{10}H_{20}$, $C_{12}H_{24}$, $C_{13}H_{26}$, $C_{14}H_{28}$, $C_{15}H_{30}$, $C_{17}H_{34}$, $C_{18}H_{36}$	C_8H_{16}, C_9H_{18}, $C_{10}H_{20}$, $C_{11}H_{22}$, $C_{12}H_{24}$, $C_{13}H_{26}$, $C_{14}H_{28}$, $C_{15}H_{30}$, $C_{17}H_{34}$, $C_{18}H_{36}$
linear alkene, n-		4-dodecene, (E)- [$C_{12}H_{24}$] 7-hexadecene, (Z)- [$C_{16}H_{32}$]	4-dodecene, (E)- [$C_{12}H_{24}$] 7-hexadecene, (Z)- [$C_{16}H_{32}$]	2-dodecene, (E)- [$C_{12}H_{24}$] 3-tetradecene, (Z)- [$C_{14}H_{28}$] 7-hexadecene, (Z)- [$C_{16}H_{32}$]
linear aldehyde	$C_{16}H_{32}O$	$C_{16}H_{32}O$	$C_{16}H_{32}O$	$C_{16}H_{32}O$
		TBOPBr		
alkane, 1-bromo		C_4H_9Br, $C_{18}H_{37}Br$	C_4H_9Br, $C_{15}H_{21}Br$, $C_{18}H_{37}Br$	C_4H_9Br, $C_{15}H_{21}Br$, $C_{18}H_{37}Br$
linear alkene, 1-		$C_{17}H_{34}$, $C_{18}H_{36}$	C_8H_{16}, $C_{11}H_{22}$, $C_{15}H_{30}$, $C_{18}H_{36}$	C_8H_{16}, $C_{11}H_{22}$, $C_{15}H_{30}$, $C_{18}H_{36}$
phosphine		$C_{12}H_{27}P$	$C_{12}H_{27}P$	$C_{12}H_{27}P$
		P-4Ph		
aryl	biphenyl [$C_{12}H_{10}$]	biphenyl [$C_{12}H_{10}$]	biphenyl [$C_{12}H_{10}$]; o-terphenyl [$C_{18}H_{14}$]; m-terphenyl [$C_{18}H_{14}$]	biphenyl [$C_{12}H_{10}$]; acenaphthene [$C_{12}H_{10}$]; o-terphenyl [$C_{18}H_{14}$]; m-terphenyl [$C_{18}H_{14}$]; p-terphenyl [$C_{18}H_{14}$]; triphenylene [$C_{18}H_{12}$]
phosphine	phosphine, triphenyl [$C_{18}H_{15}P$]	phosphine, triphenyl [$C_{18}H_{15}P$]	phosphine, triphenyl [$C_{18}H_{15}P$]	phosphine, triphenyl [$C_{18}H_{15}P$]
phosphine oxide		triphenylphosphine oxide [$C_{18}H_{15}OP$]	triphenylphosphine oxide [$C_{18}H_{15}OP$]	triphenylphosphine oxide [$C_{18}H_{15}OP$]
		TPhPBr[a]		
benzene, bromo		C_6H_5Br	C_6H_5Br	C_6H_5Br 1,1′-biphenyl, 2-bromo- [$C_{12}H_9Br$]
aryl		biphenyl [$C_{12}H_{10}$]	biphenyl [$C_{12}H_{10}$]	biphenyl [$C_{12}H_{10}$]; o-terphenyl [$C_{18}H_{14}$]; triphenylene [$C_{18}H_{12}$]
phosphine		phosphine, triphenyl [$C_{18}H_{15}P$]	phosphine, triphenyl [$C_{18}H_{15}P$]	phosphine, triphenyl [$C_{18}H_{15}P$]

[a] The reaction temperature for TPhPBr is 310 °C.

Scheme 1

$$R_3P \;+\; X\!-\!CH_2\!-\!CH_2\!-\!R' \quad \textbf{(1)}$$

$[S_N(C)]$ $X^{\ominus}$

$$R_3P{=}CH\!-\!CH_2\!-\!R' + BH \quad \textbf{(4)} \quad \xleftarrow[\;\mathbf{E_\alpha}\;]{B^{\ominus}} \quad R_3\overset{\oplus}{P}\!-\!CH_2\!-\!CH_2\!-\!R' \quad \xrightarrow[\;\mathbf{E_\beta}\;]{B^{\ominus}} \quad R_3P + CH_2{=}CH\!-\!R' + BH \quad \textbf{(2)}$$

$[S_N(P)]$ $OH^{\ominus}$

$$\underset{R_3P\!-\!CH_2\!-\!CH_2\!-\!R'}{O\text{–}H}$$

$$R_3P{=}O \;+\; CH_3\!-\!CH_2\!-\!R' \quad \textbf{(3)}$$

anion (e.g., a halide) displaces a triphenylphosphine group. This is effectively the reverse of the quaternization reaction.[31] Because there is a change in oxidation state from the reactant (P at +5 oxidation state) to the product (P at +3 oxidation state), this reaction can also be regarded as a reductive elimination process. (2) β-Elimination,[32] E_β: where the β-proton is abstracted by a base in concert with the expulsion of triphenylphosphine from the α-carbon. (3) Substitution at phosphorus,[33] **[$S_N(P)$]**: where a hydroxyl anion attacks the phosphorus center to form a five-coordinate intermediate, followed by comconmitant separation of a phosphone oxide and an alkane. This reaction is primarily driven by the formation of a strong phosphoryl (P=O) bond. (4) α-Elimination,[34] E_α: which is actually an α-proton abstraction process and the basis for the synthetically useful reaction for converting carbonyl compounds to olefins (Wittig reaction). However, this reaction typically requires a strong base such as alkyllithium or aryllithium reagents. Thus, reactions 1−3 are most likely to occur as the primary processes during

(31) Goldwhite, H. *Introduction to Phosphorus Chemistry*; Cambridge University Press: Cambridge, 1981; pp 57−68.
(32) Fenton, G. W.; Ingold, C. K. *J. Chem. Soc.* **1929**, 2342.
(33) Hey, L.; Ingold, C. K. *J. Chem. Soc.* **1933**, 531.

(34) Wittig, G.; Geissler, G. *Ann. Chem. Liebigs* **1953**, *580*, 44. Schollkopf, U. *Angew. Chem.* **1959**, *71*, 260.

Scheme 2
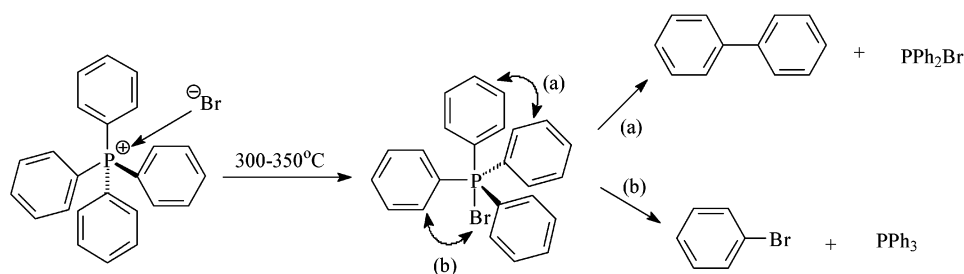
Scheme 3
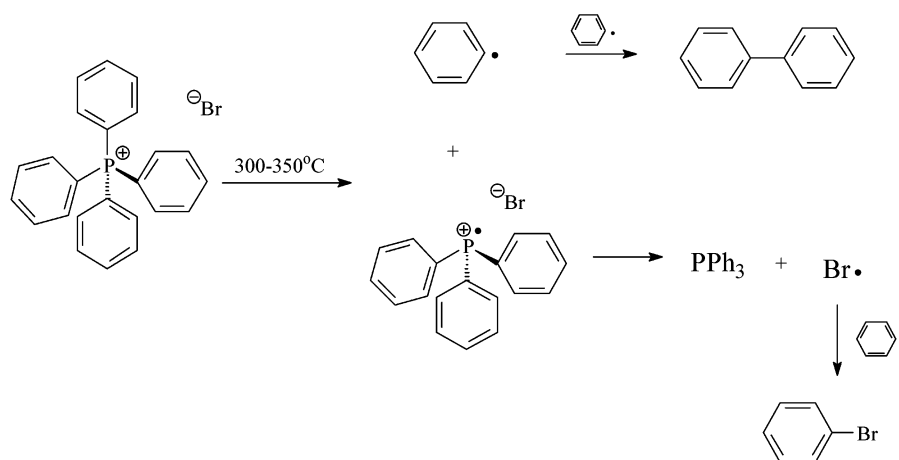
the thermal decomposition of quaternary phosphonium compounds either in neat state or intercalated within montmorillonite. Indeed, the pyrolysis/GC-MS of neat phosphonium salts indicated that both [$S_N(C)$] and E_β elimination reactions are involved, confirmed by the presence of both alkenes and alkyl (or aryl) halides in the pyrolysis products. However, the [$S_N(C)$] reaction is probably more favored in neat phosphonium salts at lower temperatures, considering the initial attack of the halide anion on the β-hydrogen is unfavored.[35, 36]

Similar to the pristine salts, tertiary phosphine and long-chain olefins are observed as the decomposition products from the alkyl P-MMTs (e.g., P-C18), but at lower temperatures (250 vs 300 °C). This indicates the occurrence of a β-elimination mechanism upon degradation of P-MMT. Additionally, phosphine oxide and octadecane are also detected from P-C18, consistent with the [$S_N(P)$] pathway associated with hydroxyls along the sheet edge.[37] The absence of alkyl halides indicates that the [$S_N(C)$] reaction is suppressed by the removal of the bromide anion and replacement by the aluminosilicate sheet. The neat negative charge of the aluminosilicate is dispersed over numerous bridging oxygen, depending on the crystallographic location of

the isomorphic substitution.[38] The weak Lewis basicity of the siloxane surface is thought to be insufficient to drive the $S_N(C)$ reaction.

In the case of tetraphenyl phosphonium, the primary thermal degradation mechanisms are expected to be different from the reaction pathways discussed above for the tetraalkyl analogues because of the following two reasons. First, the absence of α-hydrogen in the phenyl substituents precludes the occurrence of α-elimination process. Second, the β-elimination process necessitates the formation of benzyne whose formation is not favored energetically and requires the presence of a base much stronger than a hydroxide anion. Furthermore, at temperatures >300 °C, reaction pathways involving reactive intermediates, namely free radicals, are more probable. Thus, in the case of the neat salt, two possible reaction mechanisms may lead to the formation of bromobenzene, biphenyl-, and triphenylphosphine as the thermal decomposition products. The first mechanism invokes the intermediacy of five-coordinate bromotetraphenylphosphorane (Scheme 2) that rapidly undergoes reductive elimination to form the resultant products that were observed, except PPh$_2$Br, which might be unstable under the conditions and dissociate into PPh$_2$ radical and Br atom. Both can combine with phenyl radicals to form triphenylphosphine and bromobenzene. The second mechanism involves the homolysis of the P–phenyl bond to generate triphenylphosphonium radical and phenyl radical, which can subsequently either combine with another phenyl radical to form biphenyl or a bromine atom to form PhBr (Scheme 3). The bromine atom is produced from the reduction of

(35) Cristau, H. J.; Plenat, F. In *The Chemistry of Organophophorus Compounds, Vol. 3*; John Wiley and Sons: New York, 1994; pp 47–183.

(36) Claereboudt, J.; Claeys, M.; Geise, H.; Gijbels, R.; Vertes, A. *J. Am. Soc. Mass. Spectrom.* **1993**, *4*, 798.

(37) Phosphine oxide was observed in the pyrolysis of all four alkyl PMMTs and was absent in the corresponding neat phosphonium salts. Although water is a pyrolysis product, its evolution occurs before 200 °C (and the onset of phosphonium degradation), suggesting that it is not responsible for the formation of the oxide. Specifically, phosphine oxide is not observed till 250 °C and increases in relative concentration to phosphine with increasing temperature.

(38) Bleam, W. F.; Hoffmann, R. *Inorg. Chem.* **1988**, *27*, 3180–3186. Bleam, W. F.; Hoffmann, R. *Phys. Chem. Miner.* **1988**, *15*, 398–408.

Scheme 4
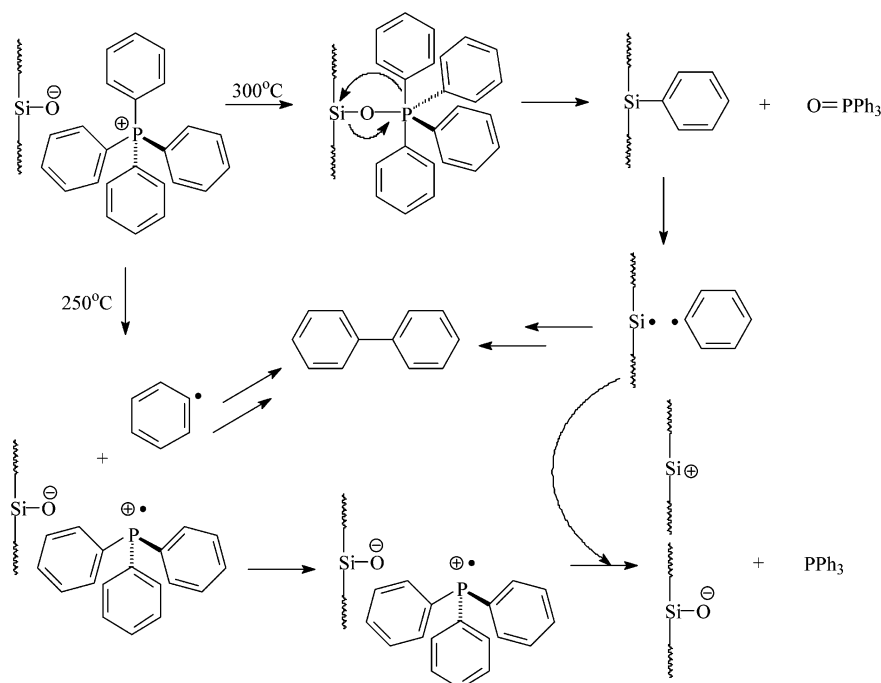
the triphenylphosphonium radical to triphenylphosphine by the attendant bromide.

Similar primary reaction mechanisms involving free radicals may be occurring when the tetraphenyl phosphonium is intercalated in montmorillonite. This is based on the fact that the expected products (PPh_3 and biphenyl) were observed in the temperature range 250–350 °C. In addition, the fact that benzene and phenol were not observed among the thermal degradation products led us to propose an additional pathway as depicted in Scheme 4 to explain the generation of triphenylphosphine oxide. In essence, this pathway is similar to the [$S_N(P)$] pathway described before for the tetraalkylphosphonium salts except that the phenyl substituent migrates to a silicon on the edge or at a defect site on the surface of montmorillonite with the concomitant release of triphenylphosphine oxide. Rapid homolytic cleavage of Si–phenyl bond generates the phenyl radical and a silicon-based free-radical on the montmorillonite. The recombination of two phenyl radicals results in biphenyl product and the latter immobilized free-radical can conceivably reduce the nearby triphenylphosphosphonium radical to triphenylphosphine. Although the phenyl-migration step is driven by the formation of the phosphoryl bond, it occurs at higher temperatures (≥ 300 °C) because the Si–O bond (111 kcal/mol) is relatively strong in comparison to the P=O bond (~ 130 kcal/mol)[39] formed. The need to form a P=O bond in order to energetically compensate for the breaking of a strong Si–O bond also provides the rationale for the migration of the phenyl group to silicon instead of oxygen. The migration of phenyl group to oxygen has been documented in the solution reaction of triphenylalkylphosphonium iodides ($Ph_3PR^+ I^-$) with methoxide, resulting in the isolation of Ph_2PR and

PhOMe (anisole).[40] The absence of phenol among the thermal degradation products lends support to the proposed phenyl-migration step.

As the temperature increases (400 °C), shorter tertiary phosphines are observed along with shorter chain olefins, branched olefins, and aldehydes. This implies that after the initial decomposition step the evolved products, which are confined inside the montmorillonite's lamallar crystal structure, undergo additional and successive secondary reactions (olefinic addition, alkyl chain scission, and condensation) at higher temperatures. Furthermore, the presence of metallic species, such as Fe^{3+} and Fe^{2+}, within the montmorillonite layer may serve as catalysts to enable the oxidative cleavage of alkenes to produce aldehydes.

Discussion

The decreased thermal stability, staged decomposition process, and different products imply that the thermal decomposition process of phosphonium cations within montmorillonite follows multiple reaction pathways due to the catalytic and morphological effects of the aluminosilicate matrix.

In general, the nonisothermal decomposition behavior for P-MMT and N-MMT share similar characteristics. β-Elimination and nucleophilic substitution occur in both cases. Additionally, the multistep decomposition implies that the presence of the nanoscopic dimensions of the interlayer greatly affects reaction kinetics and product transfer, ultimately resulting in a substantial carbonaceous yield. The major difference between the thermal decomposition behavior for P-MMT and N-MMT is that the maximum rate of mass loss and onset temperature for neat phosphonium salts are consistently 70–80 °C higher than that observed in the corresponding P-MMT, whereas only a 15–25 °C dif-

(39) Corbridge, D. E. C. *Phosphorus: An Outline of its Chemistry, Biochemistry and Technology*; Elsevier Science Publishers: Amsterdam, The Netherlands, 1990; p 44.

(40) Grayson, M.; Keough, P. T. *J. Am. Chem. Soc.* **1960**, *82*, 3919.

ference is observed between neat ammonium salts and the corresponding N-MMT, indicating that the influence of the layered silicate is more substantial for phosphonium than ammonium surfactants. At this point there are insufficient data to specifically ascribe the observed catalytic effect to translational confinement or to specific crystallographic sites or defects in the aluminosilicate. Previous work showed that when the anion of the phosphonium is hydroxide the first products of pyrolysis were detected at lower temperatures than when halides were the anion.[41] This phenomenon was attributed to the formation of the highly stable P=O bond (phosphine oxide). The ammonium salts, however, cannot decompose by a substitution mechanism to produce amine oxide because the nitrogen atom has no vacant d orbitals of low enough energy to form a five-coordinate intermediate. As a result, phosphonium salts can be more easily attacked by edge OH and thus more susceptible to catalytic effects than ammonium salts.

Nevertheless, higher thermal stability is observed from P-MMT than N-MMT, irrespective of the additional effects of the aluminosilicate. Because the thermal stability of exchanged MMT is related to the thermal stability of the parent salts, the much higher initial decomposition temperature of the parent phosphonium salts compared to the ammonium salts compensates for the loss due to the influence of the aluminosilicate.

In contrast to previous studies on N-MMTs, the architecture of the phosphonium cation is reflected in the thermal stability of the P-MMTs. Comparison of P-C14, P-C16, and P-C18 indicates that the alkyl chain length does not influence the thermal stability of corresponding P-MMTs (Figure 2b, Table 2), paralleling previous observation from alkyl N-MMTs and in agreement with the anticipated decomposition reactions. However, the stability of a longer chain, symmetric alkyl P-MMT, such as P-4C8, is ~30 °C greater than that of tributyl alkyl phosphonium MMTs, even though the stability of the salt is only slightly greater (0−5 °C). Similar dependence on architecture is not observed for N-MMTs. The initial decomposition temperature for tetraoctyl quaternary ammonium modified montmorillonite (N-4C8) and the corresponding salt is similar to that of other trimethyl alkylammonium MMTs and salts.[9] The increased stability of P-4C8 probably reflects increased steric resistance around the P center inhibiting the bimolecular reactions at the P [$S_N(P)$] or the β-C [E_β]. The substantially greater stability of the tetraaryl phosphonium arises from the alternative decomposition pathways. When aryl akyl phosphonium is present, such as triphenyl alkyl montmorillonite (P-C12), lower stability (~20 °C) relative to tetraaryl phosphonium is observed. Nonetheless, the stability is ~15 °C greater than tetraalkyl P-MMTs. The steric hindrance provided by the phenyl group is probably the major contributor to this behavior. Alternatively, the possibility of pπ−dπ interactions between the P and phenyl groups, resulting in the delocalization of the positive charge can also diminish the susceptibility of the alkyl chain to β-elimination, increasing the thermal stability of P-C12.

Morphologically, these studies indicate that four distinct interlayer environments are present between room temperature and interlayer collapse, which subdivide the initial two major degradation regions ascribed by DTG (Figure 1, Regions I and II). From room temperature to 70 °C, the interlayer contains solid-like, paraffinic surfactants (i).[22] Subsequently, melting of the long chain alkyls results in a dynamic, liquid-like interlayer (ii). Depending on the chain length, architecture, and surfactant density the first environment may not occur. At temperatures around 200 °C, decomposition of the surfactant begins in the vicinity of the P (or N) resulting in an interlayer containing small volatile and long chain molecules that are not associated with the aluminosilicate layer (iii). Finally, complete evolution of decomposition products at temperatures in excess of 350−380 °C leads to gallery collapse and the retention of a substantial fraction of organic mass as carbonaceous char (iv).

The presence of environments iii and iv is not well appreciated in the literature. The creation of mobile products, from a surfactant initially translationally confined within the interlayer, may provide an additional entropic driving force for polymer intercalation. In contrast, the disappearance of the compatibilization between the aluminosilicate and polymer will inhibit polymer inclusion. The role of these products in nanocomposite formation has not been considered and future studies are required. Furthermore, in some instances the decomposition products, such as the acidic proton arising from β-elimination, may serve to further degrade other organic moieties near the aluminosilicate surface, effectively creating a self-catalyzing decomposition. Finally, the enhanced carbonaceous yield must influence the self-passivation response[7,42] and enhanced flammability[10] characteristics of PLSNs. However, minimal information is available on the impact of layered silicate morphology, whether simply organically modified layered silicate or dispersed in a polymer, on the extent to which carbonaceous yield is enhanced.

Conclusion

In summary, the superior improvement in thermal stability for P-MMT compared to that of N-MMT, along with the well-known properties of phosphorus compounds, such as flame retardancy and heat stabilization, are advantages to the utilization of P-MMT in various polymer nanocomposites. In contrast to N-MMTs, the degradation pathways and thermal stability depend on surfactant architecture. The stability though is substantially decreased (70−80 °C) with regard to the parent phosphonium salt, necessitating future studies of the specific influence of the interlayer environment and aluminosilicate surface on reaction pathways.

(41) Abraham, S. J.; Criddle, W. J. *J. Anal. Appl. Pyrol.* **1985**, *7*, 337.

(42) Fong, H.; Vaia, R. A.; Sanders, J. H.; Lincoln, D.; Vreugdenhil, A. J.; Liu, W.; Bultman, J.; Chen, C. *Chem. Mater.* **2001**, *13*, 4123.